대형지진시험구조물의 지진응답해석
Earthquake Response Analysis of A Large Scale Seismic Test Structure

윤정방* 박경래** 김재민***
Yun, Chung-Bang Park, Kyoung-Lae Kim, Jae-Min

ABSTRACT

This paper presents the earthquake response analysis results on the Large-Scale Seismic Test (LSST) structure which was built at Hualien in Taiwan. The seismic analysis is carried out using a computer code KIESSI, which has been developed based on the three-dimensional axisymmetric finite element method incorporating infinite elements for the far field soil region. The soil and structural properties obtained from the post-correlation study of the forced vibration tests (FVT) are utilized to predict seismic responses. The ground accelerations recorded at a site 56.5 m from the test structure are used as control motions. It has been found that the predicted responses are reasonably compared with the observed responses.

1. INTRODUCTION

An international collaboration research among researchers from Korea, Japan, Taiwan, USA and France has been conducted for the investigation of the soil-structure interaction (SSI) effects during strong earthquake events and also for the verification of the SSI analysis programs using the measured earthquake responses. A 1/4-scale model of a PWR type reactor containment building was constructed at Hualien in Taiwan, where the high seismic activity is high [1]. The blind prediction and post-correlation analysis for FVT has been performed [2]. In this paper, the earthquake response analysis results using the FVT-correlated properties of the structure and soil medium are presented.

The predictions for the seismic responses of the structure and the surrounding soil are carried out by a direct approach incorporating the finite element and infinite element methods and using the substructured wave input technique. At first, free-field responses on the interface between the near and far fields are obtained by deconvolving the given earthquake acceleration (control motion). A computer program FREE which has been developed by the dynamic stiffness matrix method [3] is used. Based on the free-field analysis results, the equivalent earthquake forces along the interface are calculated. Then the earthquake responses are obtained at the several sensor locations on the structure and the ground surface using the computer program KIESSI [4]. The substructured wave input procedure [5] is adopted in the present analysis.

* 한국과학기술원 토목공학과 교수
** 롯데건설 연구원
*** 한국과학기술원 토목공학과 박사과정

2. FREE-FIELD ANALYSIS

In the dynamic stiffness matrix method, the free-field soil medium is assumed to be a horizontally layered halfspace and the seismic waves are assumed to be plane body waves. Then the dynamic equilibrium equation in each layer can be represented as [3]

$$\mathbf{K}_m(\omega)\, \mathbf{u}_{(m)}(\omega) = \mathbf{f}_{(m)}(\omega) \qquad (m = 1, 2, \ldots, n) \tag{1}$$

in which $\mathbf{K}_m$ is the frequency-dependent dynamic stiffness matrix of the m-th layer, $\mathbf{u}_{(m)}$ and $\mathbf{f}_{(m)}$ are the displacement and traction vectors on the upper interface of the m-th layer, respectively, and n is the number of layers including the underlying halfspace. The dynamic equilibrium equation of the whole free-field system can be obtained by assembling the above equations as

$$\mathbf{K}_{total}(\omega)\, \mathbf{u}_{total}(\omega) = \mathbf{f}_{total}(\omega) \tag{2}$$

Therefore, if the control motion is given on any layer interface, the motions on the other layer interfaces can be computed by solving the above equation .

The free-field analysis for the Hualien LSST site is performed using the unified soil model consisting of Sand-1, Sand-2, Gravel-3 and Gravel-4 layers as shown in Fig. 1. The properties of the unified soil model are shown in Table 1. The soil profile and the sensor locations in the soil are shown in Fig. 1 and Fig. 2, respectively. The earthquake time histories measured at point A15 on the ground surface on Jan. 20, 1994 are used as control motions (Fig. 3). The peak accelerations of the control motions are 0.0318g in the NS-direction and 0.0444g in the EW-direction. The soil is assumed to be linear since the magnitude of the control motion is judged to be small enough to ignore the nonlinearity of the soil medium.

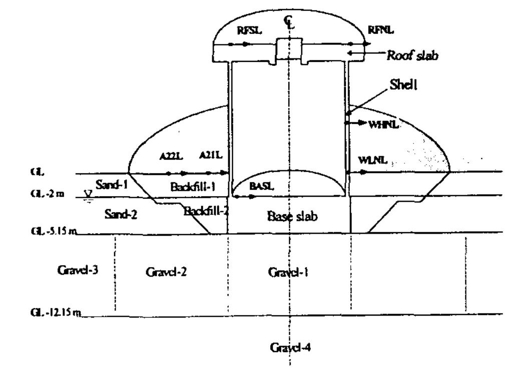

Fig. 1 The soil-structure system and sensor locations

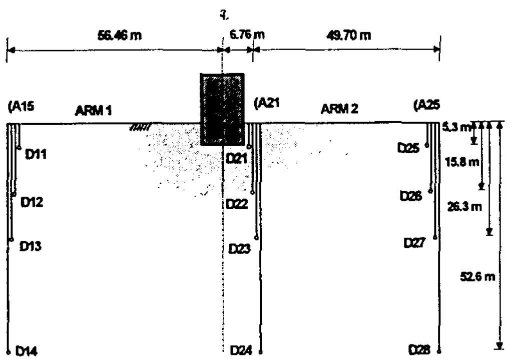

Fig. 2 The sensor locations in the soil medium

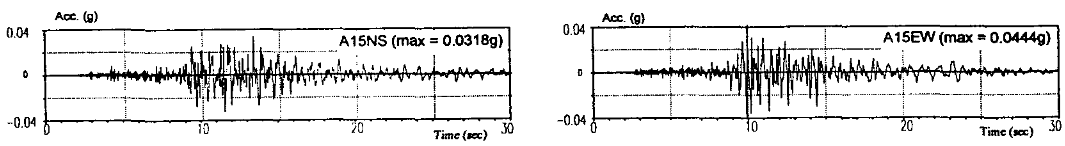

(a) NS-direction

(b) EW-direction

Fig. 3 Measured accelerations at A15 used as control motions in free-field analysis

Table 1. The properties of the soil layers and structure (units : V_S in m/sec and E in GPa)

Partitioned Regions	Mass density, ρ (ton/m^3)	Damping ratio, h	Poisson's ratio, ν	V_s for soil or E for structure	
				Unified model	FVT-correlated model
Sand-1	1.69	0.02	0.38	133	133
Sand-2	1.93	0.02	0.48	231	231
Backfill-1	2.33	0.02	0.38	400	310
Backfill-2	2.39	0.02	0.48	400	340
Gravel-1	2.42	0.02	0.47	383	340
Gravel-2	2.42	0.02	0.47	333	280
Gravel-3	2.42	0.02	0.47	333	333
Gravel-4	2.42	0.02	0.47	476	428
Roof & Base	2.57	0.02	0.167	28.2	28.2
Shell	2.57	0.02	0.167	28.2	22.0

The time histories and the response spectra calculated at several downhole sensor locations are compared with the measured ones in Figs. 4 and 5. The results of the free-field analysis indicate that the unified soil model gives very good results in the NS-direction but fairly large discrepancies in the EW-direction. In case of the EW-direction, the calculated response is consistent with the observed data at D11 (GL-5.26 m). However, there are large differences between the observed data and the calculated responses using the unified soil model at the downhole sensor locations below D11 (i.e., D12 and D13). This result indicates that the soil properties of the first sublayer underneath the structure are considerably different from those of the unified model in the EW-direction. Thus, it can be concluded that the soil layer between GL-5.25 m and GL-15.78 m may behave anisotropically. On the other hand, the sand layers above GL-5.25 m can be assumed to be assumed to be isotropic, because the calculated free-field responses in both directions are consistent with the measured data.

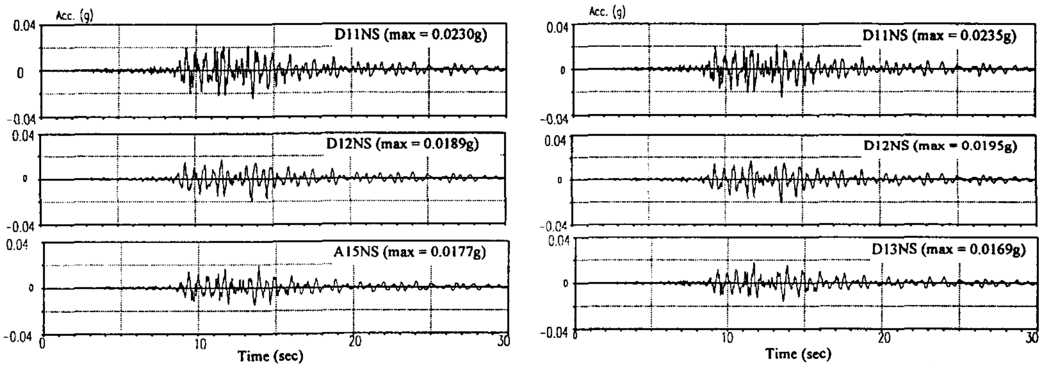

(a) Observed accelerations (b) Calculated accelerations

Fig. 4 The observed and calculated accelerations at downhole locations in the NS-direction

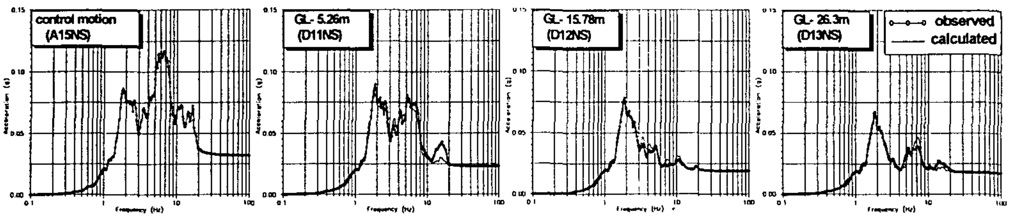

(a) NS-direction (A15NS = control motion)

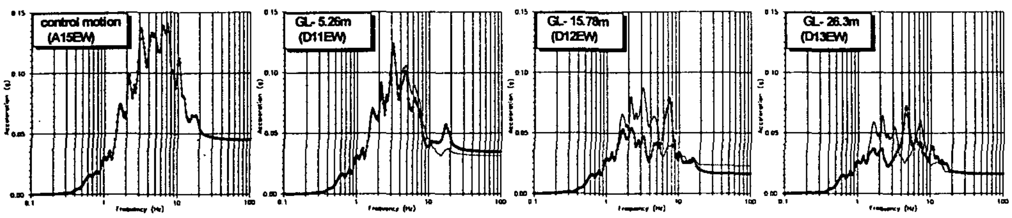

(b) EW-direction (A15EW = control motion)

Fig. 5 Response spectra of the observed and calculated accelerations at downhole locations (ξ = 5%)

3. EARTHQUAKE RESPONSE ANALYSIS

In this study, responses to the earthquake loadings have been obtained by solving the following wave radiation equation as

$$\begin{bmatrix} \mathbf{K}_{nn}(\omega) & \mathbf{K}_{ni}(\omega) \\ \mathbf{K}_{in}(\omega) & \mathbf{K}_{ii}(\omega)+\overline{\mathbf{K}}_{ii}(\omega) \end{bmatrix} \begin{Bmatrix} \mathbf{u}_n(\omega) \\ \mathbf{u}_i(\omega) \end{Bmatrix} = \begin{Bmatrix} \mathbf{0} \\ \mathbf{f}_i(\omega) \end{Bmatrix} \tag{3}$$

in which the subscripts n and i denote the degrees of freedom in the near and far field regions, respectively; $\overline{\mathbf{K}}_{ii}$ is the dynamic stiffness matrix of the far field region which can be easily obtained by the infinite element formulation; and $\mathbf{f}_i$ is the equivalent earthquake force along the interface boundary Γ_i as shown in Fig. 6, which can be calculated as [5]

$$\mathbf{f}_i(\omega) = \overline{\mathbf{K}}_{ii}(\omega)\,\bar{\mathbf{u}}_i(\omega) - \mathbf{A}\,\bar{\mathbf{s}}_i(\omega) \tag{4}$$

where $\bar{\mathbf{u}}_i$ and $\bar{\mathbf{s}}_i$ are the respective displacement and stress on Γ_i obtained from the free-field analysis, and $\mathbf{A}$ is a constant transformation matrix.

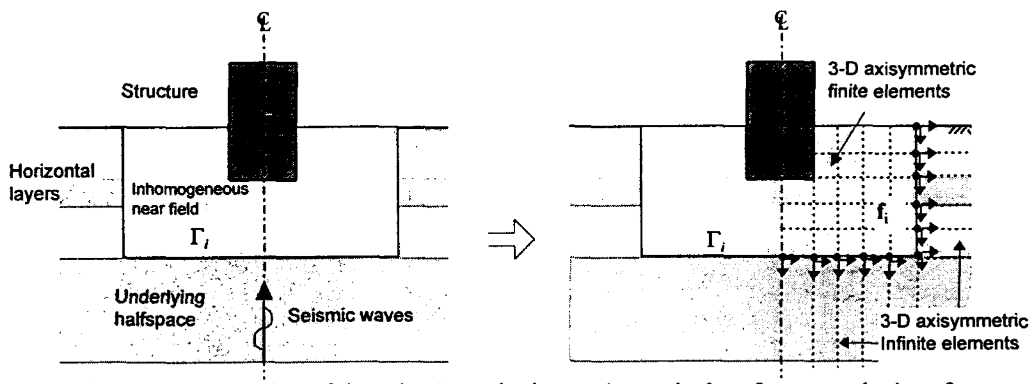

Fig. 6 Representation of the seismic excitation as the equivalent forces on the interface

For the verification of the earthquake response analysis procedure in the program KIESSI, a site-response analysis has been carried out for vertically incident SH-waves. The finite element mesh and the selected points for response evaluations are shown in Fig. 7. The acceleration of A15NS shown in Fig. 3(a) is used as the control motion on the ground surface. Comparisons shown in Fig. 9 indicate that the calculated earthquake responses are almost identical to those of the free-field analysis.

Earthquake responses to the NS- and EW-excitations are calculated by utilizing the unified and the FVT-correlated soil-structure models [2]. The properties of the FVT-correlated model are shown in Table 1 and the finite element mesh in Fig 8. Since the estimated soil responses in the NS-direction from the free-field analysis show good agreements with the measurement data while those in the EW-direction show poor comparisons, the earthquake response analysis is carried out mainly for the NS-direction. The response spectra and the transfer functions are obtained and compared with the observed ones in Fig. 10 and Fig. 11, respectively. The first natural frequency evaluated from the earthquake response data is 5.3 Hz, while those from the analysis are 7.2 and 6.2 Hz for the cases with the unified and the FVT correlated models, respectively. The fundamental natural frequency from the previous FVT test after backfill was 6.1 and 6.3 Hz in the two principle directions. The discrepancy between the natural frequencies from two sets of test data may be caused by the nonlinear and anisotropic behavior of the soil medium near the structure. In general, the predicted responses using the FVT correlated model show better agreements with the measured responses than those using the unified model. The calculated responses at the lower levels of the structure (BAS and WLN) and on the ground surface (A21 and A22) show better agreements with the measured data, while those at the upper levels of the structure (RFN and WHN) are found to be significantly larger than the measured data particularly in the high frequency range. It may be because the damping has been underestimated for the rocking mode in the present analysis model. Further investigations are required to examine the nonlinear behavior of the soil near the structure for strong earthquake excitations.

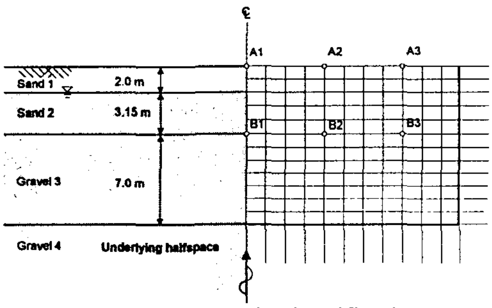

Fig. 7 Finite element mesh of verification example

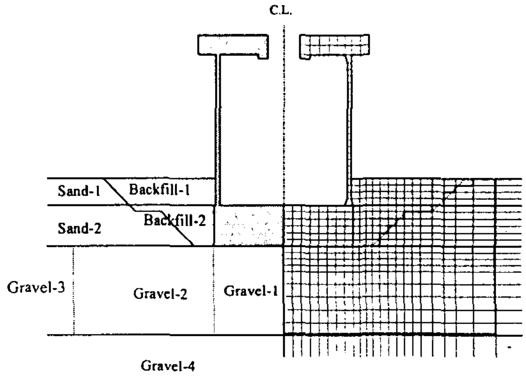

Fig. 8 Finite element mesh for Hualien LSST

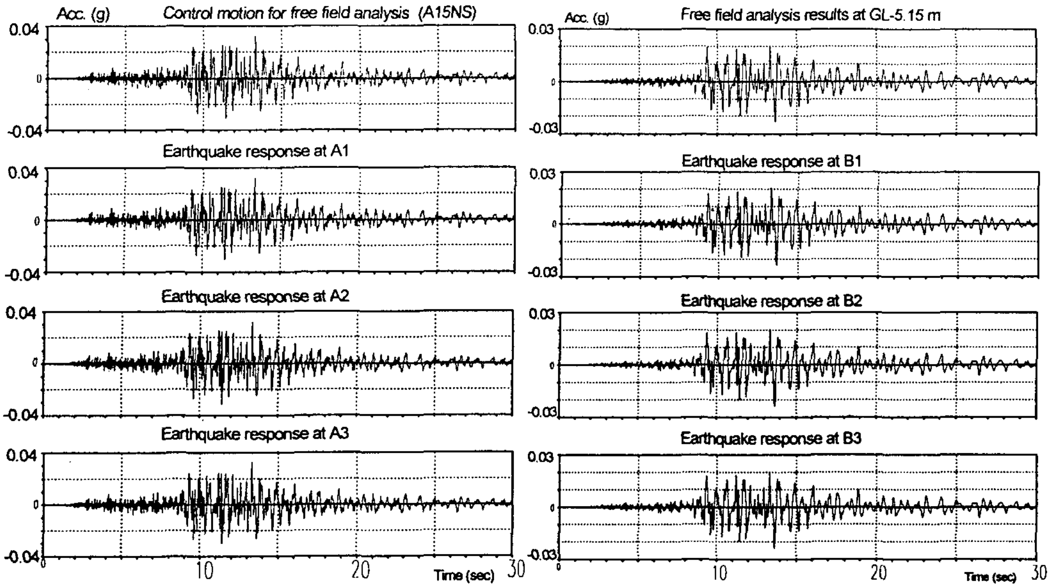

(a) at ground level (b) at level GL-5.15m

Fig. 9 Comparison of earthquake responses in soil with free-field analysis results

4. CONCLUSIONS

Based on the present analysis results, the following conclusions are made :

(i) The free-field analysis results show good agreements with the recorded data in the NS-direction but poor results in the EW-direction. It appears that the anisotropy of soil medium exists especially in the layer between GL-5.25 m and GL-15.78 m.

(ii) Acceptable earthquake responses are obtained at the lower levels of the structure and on the ground surface using the FVT-correlated model. However relatively larger responses are predicted at the upper levels of the structure particularly for the high frequency excitations. High responses may be caused by the underestimation of the damping for the rocking motion in the present analysis model.

(iii) Since the fundamental frequency of the earthquake response becomes smaller than that of the FVT and the shape of transfer functions bends to the left, the nonlinearity in the soil medium seems significant in spite of the small magnitude of the earthquake excitation (PGA=0.032 g).

(iv) Further investigations are required on the soil-structure model and the nonlinear behaviors of the soil medium during strong earthquakes.

ACKNOWLEDGMENT

The authors would like to thank the Korea Institute of Nuclear Safety and the Ministry of Science and Technology for the financial support.

REFERENCES

1. Tang, H.T., Stepp, J.C., *et al*, "The Hualien large-scale seismic test for the soil-structure interaction research", *Proc. 11th SMiRT*, 1991, K1, pp 69-74.
2. Yun, C.B. and Kim, J.M., "Post-correlation Analysis for FVT after Backfill of Hualien LSST Project", *TMC/EOC Meeting for Hualien Project*, France, June, 1994.
3. Wolf, J. P., *Dynamic Soil-Structure Interaction*, Prentice-Hall, 1985.
4. Yun, C.B., Kim, J.M. and Hyun, C.H., "Axisymmetric elastodynamic infinite elements for multi-layered halfspace", *Int. J. Num. Meth. Engng*, in press, 1995.
5. Zhao, C. and Valliappan, S., An efficient wave input procedure for infinite media, *Communications in Numerical Methods in Engineering*, 1993, 407-415.
6. Park, K.L., "Seismic analysis of soil-structure interaction system incorporating infinite elements", *Msc. Thesis*, Dept. of Civil Engng, KAIST, Feb., 1995.

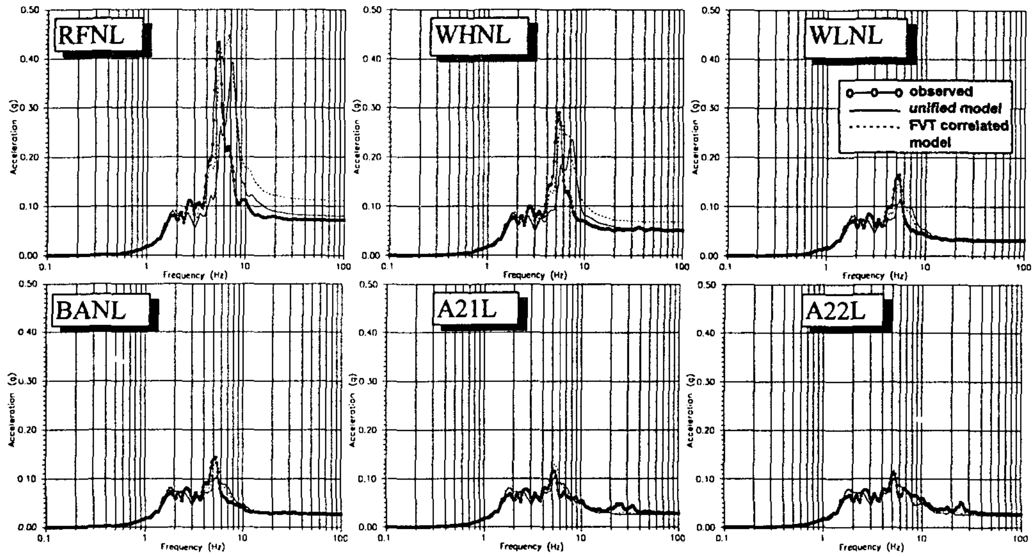

Fig. 10 Response spectra at several locations in the NS-direction

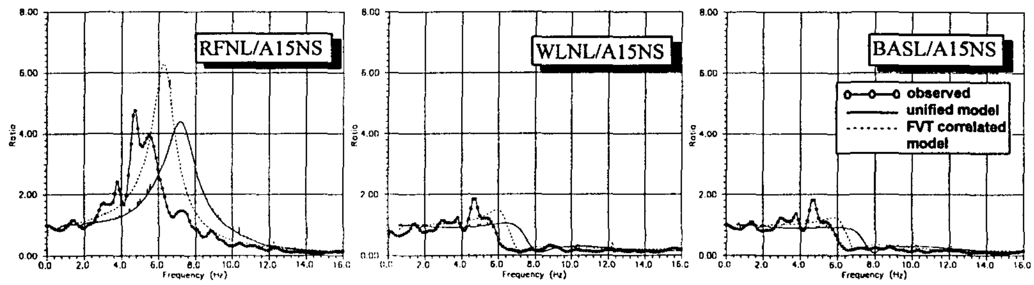

Fig. 11 The transfer functions of accelerations in the NS-direction